Chemical Engineering Journal 126 (2007) 171–180

Chemical Engineering Journal

www.elsevier.com/locate/cej

Analytical solution of gravity separation model (GSM): Separation of water droplets from vapor in submerged combustion evaporator

Dongbei Yue *, Yudong Xu, Rasool Bux Mahar, Fuqiang Liu, Yongfeng Nie

Department of Environmental Science and Engineering, Tsinghua University, Beijing 100084, China

Received 8 September 2005; received in revised form 28 August 2006; accepted 12 September 2006

Abstract

As a kind of direct contact heating method, submerged combustion evaporator (SCE) has many advantages and is widely used in many engineering processes. The entrainment of water droplets in vapor significantly affects the separation efficiency of SCE with sparkling of hot gases. In order to ensure high evaporation efficiency, it is necessary to minimize water droplets containing high concentration of pollutants. Vapor separation space provides place for water droplets separating from vapor by gravity. Therefore, it is very important to study the gravity separation behavior of water droplets from vapor. Gravity separation model (GSM) for water droplets separation from vapor is elaborated in this paper, and its analytical solution for this model is described. Based on this model and its analytical solution, the effects of the gravity separation height and velocity of the vapor flow on the separation efficiency are discussed in details. It corresponds well with the existing numerical results. The results show that, all the droplets decelerate after entering the vapor flow; and it is not necessary to increase the height of gravity separation space after getting maximum separation efficiency. For the same height of gravity separation space, separation efficiency decreases with vapor velocity increasing. At constant vapor velocity, the maximum efficiency of separation for different initial velocities of droplet is the same. And the faster the initial velocity, the higher space for gravity separation is needed to get the maximum efficiency. This model could be used for the improvement of separation efficiency of SCE and optimization of its design.

Keywords: Gravity separation; Separation efficiency; Submerged combustion evaporator

1. Introduction

Submerged combustion [1,2] is a kind of heating method by direct contact of the flame or hot gases from a burner with a fluid or liquid substance such as water, oil or tar. The first record of submerged combustion evaporator is described in the British patent specification granted to Collier in 1886 (Fig. 1). This early attempt embodied nearly all the best features of the modern submerged combustion evaporator. Compared with conventional recuperative heat exchanger, the submerged combustion evaporator (SCE) has many obvious advantages [1,3,4] such as no fixed interface, direct contact, high speed and efficiency for the heat transfer. So, currently, the SCE is widely used in nuclear engineering, steel engineering [3], chemical engineering [5,6], environmental engineering [7–9] and other engineering processes, for evaporation, concentration and separation of target liquid or solution, especially for scale formation solution, for instance, with the treatment of sanitary landfill leachate [10–12].

Generally, entrainment of water droplets holding high concentration of chemical substances greatly influences the separation efficiency of evaporator and pollutes the environment. In order to ensure high evaporation separation efficiency, it is necessary to minimize water droplet content in the vapor. Vapor separation space provides place for water droplets separating from vapor by gravity. If the adequate height of vapor separation space cannot be ensured, the exhaust gas and condensate will contain much more solute, and will contaminate the environment. On the other hand, an excessive height of vapor separation space does not improve the separation efficiency significantly but increases the manufacture cost. Therefore, to define the reasonable height of the separation

* Corresponding author at: Department of Environmental Science and Engineering, Room 401, Tsinghua University, Beijing 100084, China.
Tel.: +86 10 6279 4697; fax: +86 10 6277 2048.
E-mail address: yuedb@tsinghua.edu.cn (D. Yue).

1385-8947/$ – see front matter
doi:10.1016/j.cej.2006.09.008

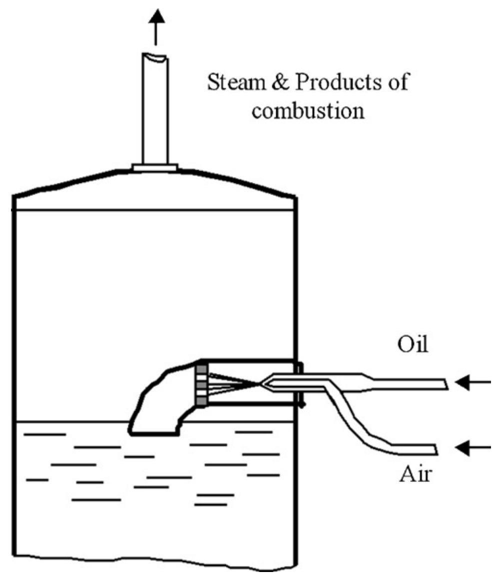

Fig. 1. The first submerged combustion evaporator.

space, it is necessary to study the movement behavior of water droplets in the vapor. However, very limited research has been conducted for investigating the phenomenon, and only numerical models were given for pressurized water reactor steam generator [13,14].

In this study, a new mathematical model is developed for gravity separation of water droplets from vapor, and an analytical solution for this model is given. Based on this model and its analytical solution, the effects of the gravity separation height as well as the velocity of the vapor flow on the gravity separation efficiency are discussed.

2. Formation and entrainment of droplets

The bubbles that consist of vapor, carbon dioxide, nitrogen, excess oxygen and some VOCs, ascend rapidly from nozzles in the liquid. When passing the liquid–gas interface, the bubble breaks down, and the broken pellicles turn into droplets. Furthermore, the collision of the surrounding liquid results in formation of larger droplets (Fig. 2). Smaller droplets formed at the interface can be carried away out of the submerged combustion evaporator. Some bigger droplets can only flow up to a certain height and then fall back down to the liquid. This height is named gravity separation height of droplet.

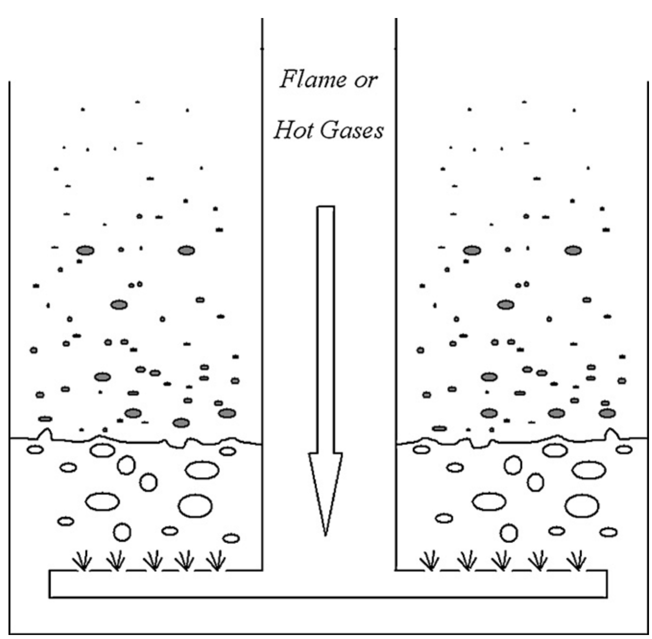

Fig. 2. Schematic diagram of formation and entrainment of droplets.

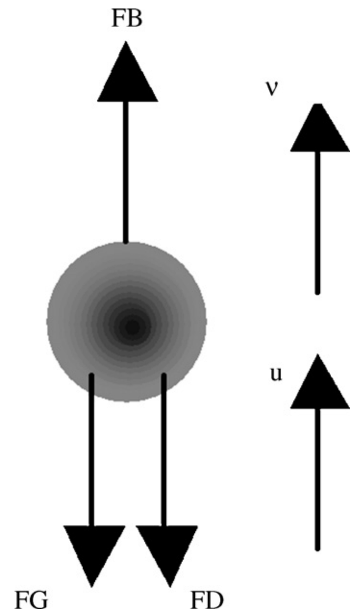

Fig. 3. Mechanical analysis of droplet: F_G, gravitational force; F_B, buoyancy force; F_D, drag force; v, velocity of droplet; u, velocity of vapor flow.

Those small droplets of which the gravity separation height exceeds the actual height of vapor separation space or even without gravity separation height (for very small droplets, the drag force of vapor can overcome their weight so that they can be carried to any height) can go with vapor out of submerged combustion evaporator. Gravity separation height is related to the following factors:

(1) Initial ascending velocity of droplet.
(2) Drag force of vapor. When the droplet is flowing up faster than vapor, the drag force obstructs it in climbing. On the contrary, when the droplet is flowing up slower than vapor or falling down, the drag force tries to take it with vapor.
(3) Velocity of vapor flow. Increasing in velocity of vapor flow can aggravate the entrainment process.

3. Gravity separation model

3.1. Fundamental assumptions

This study is based on the following assumptions:

(1) Droplets are in the shape of ball.
(2) No interaction among droplets.
(3) No vaporization and condensation with droplets.
(4) Droplet motion is of one dimension.
(5) Sectional area of the vapor separation space is constant along the height.

3.2. Droplet mechanics

The droplet's motion in the vapor flow is affected by gravity, buoyancy and drag force. The gravity and the buoyancy force make effect on the droplet with direction of downward and upward, respectively, and the relative movement between the droplet and vapor flow determines the direction of drag force (Fig. 3).

Gravity force, $F_G = \rho_s V g$,

where ρ_s is the density of droplet, V the volume of droplet, $V = \pi d^3/6$, in which, d is the diameter of droplet, and g is the gravitational accelerated speed.

Buoyancy force, $F_B = \rho V g = \rho g \dfrac{\pi d^3}{6}$,

where ρ is the density of vapor.

Drag force, $F_D = 0.5 C_D v'^2 \rho A$,

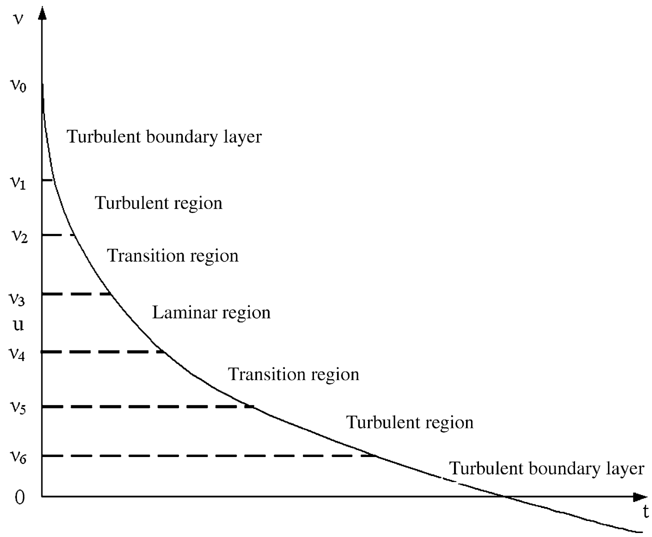

Fig. 4. Flow patterns of ascending droplet.

where v' is the relative velocity between droplet and vapor flow; A the projected area (in the direction of motion); and C_D is the coefficient of drag force, which can be calculated as the following:

$$\begin{aligned} &\text{laminar region:} \quad C_D = \frac{24}{Re}, \quad 0 < Re < 2 \\ &\text{transition region:} \quad C_D = 0.4 + \frac{40}{Re}, \quad 2 < Re < 500 \\ &\text{turbulent region:} \quad C_D = 0.44, \quad 500 < Re < 2 \times 10^5 \\ &\text{turbulent boundary layer:} \quad C_D = 0.1, \quad Re > 2 \times 10^5 \end{aligned} \tag{1}$$

where Reynolds number, $Re = |v'|d\rho/\mu$, so

$$|v'| = |v - u| = \frac{Re\mu}{d\rho}. \tag{2}$$

One certain droplet can pass through all the existing different flow patterns during its rising process shown in Fig. 4 with v decreasing from initial velocity to zero. As long as the velocity down to zero, the droplet starts to fall.where v_0 is the initial velocity of droplet.

In accordance with the ranges of Reynolds number for different flow regions, the respective velocities of droplet are expressed as:

$$\begin{aligned} v_1 &= u + \frac{2 \times 10^5 \mu}{d\rho}; \\ v_2 &= u + \frac{500\mu}{d\rho}; \\ v_3 &= u + \frac{2\mu}{d\rho}; \\ v_4 &= u - \frac{2\mu}{d\rho}; \\ v_5 &= u - \frac{500\mu}{d\rho}; \\ v_6 &= u - \frac{2 \times 10^5 \mu}{d\rho}. \end{aligned} \tag{3}$$

3.3. Development of gravity separation model and its analytical solutions

3.3.1. Governing equation

According to the summation rule, we obtain the following governing equation:

$$F_G + F_D - F_B = -m\frac{dv}{dt}. \tag{4}$$

The flying height of droplet in vapor separation space, h, can be written as:

$$h = \int v\,dt. \tag{5}$$

Note that in Eq. (4), the direction of drag force can change plus or minus, depending on the relative movement between the droplet and vapor flow, and the droplet motion initial time is always considered zero in every flow pattern, and it is assumed the initial and the final velocities of the droplet in any flow region are v_a and v_b, respectively. In Eq. (5), initial h is assumed zero in every flow region. Under these conditions, if Eq. (4) can be analytically solved to obtain function v expressed with variable t and other parameters available, i.e. $v = f(t)$, it is possible to get an analytical solution for h after substituting $v = f(t)$ into Eq. (5). This idea has been explored further in the following for every flow pattern.

It is very crucial to divide the rising process into several flow regions for analytical solutions. With the presence of mathematics handbook, the analytical solutions to Eqs. (4) and (5) within different regions are achieved.

3.3.2. Droplet upwards across turbulent boundary layer ($v_1 < v < v_0$, $C_D = 0.1$)

The relative velocity of droplet is $v' = v - u$, and the drag force downwards.According to Eq. (4), there is:

$$100(\rho_s - \rho)g + \frac{7.5\rho}{d}v'^2 = -100\rho_s\frac{dv}{dt}. \tag{6}$$

Integrating Eq. (6) gives

$$v = \left(\left(\left(\frac{100(\rho_s-\rho)dg}{7.5\rho}\right)^{1/2} + \left(\frac{100(\rho_s-\rho)dg}{7.5\rho}\right)^{3/2}\frac{1}{(v_a-u)^2}\right)\left(\tan\left(\sqrt{\frac{7.5\rho(\rho_s-\rho)g}{100d\rho_s^2}}t\right) + \frac{10}{v_a-u}\sqrt{\frac{(\rho_s-\rho)dg}{7.5\rho}}\right)^{-1} - \frac{100(\rho_s-\rho)dg}{7.5\rho}\frac{1}{v_a-u} + u \tag{7}$$

And then,

$$h = ut + \frac{100d\rho_s}{7.5\rho}\ln\left(\cos\left(\sqrt{\frac{7.5\rho(\rho_s-\rho)g}{100d\rho_s^2}}t\right) + \frac{v_a-u}{10}\sqrt{\frac{7.5\rho}{(\rho_s-\rho)dg}}\sin\left(\sqrt{\frac{7.5\rho(\rho_s-\rho)g}{100d\rho_s^2}}t\right)\right) \tag{8}$$

3.3.3. Droplet upwards across turbulent region ($v_2 < v < v_1$, $C_D = 0.44$)

According to Eq. (4), there is

$$100(\rho_s - \rho)g + \frac{33\rho}{d}v'^2 = -100\rho_s\frac{dv}{dt}. \tag{9}$$

Accordingly,

$$v = \left(\left(\left(\frac{100(\rho_s-\rho)dg}{33\rho}\right)^{1/2} + \left(\frac{100(\rho_s-\rho)dg}{33\rho}\right)^{3/2}\frac{1}{(v_a-u)^2}\right)\left(\tan\left(\sqrt{\frac{33\rho(\rho_s-\rho)g}{100d\rho_s^2}}t\right) + \frac{10}{v_a-u}\sqrt{\frac{(\rho_s-\rho)dg}{33\rho}}\right)^{-1} - \frac{100(\rho_s-\rho)dg}{33\rho}\frac{1}{v_a-u} + u \tag{10}$$

and,

$$h = ut + \frac{100d\rho_s}{33\rho}\ln\left(\cos\left(\sqrt{\frac{33\rho(\rho_s-\rho)g}{100d\rho_s^2}}t\right) + \frac{v_a-u}{10}\sqrt{\frac{33\rho}{(\rho_s-\rho)dg}}\sin\left(\sqrt{\frac{33\rho(\rho_s-\rho)g}{100d\rho_s^2}}t\right)\right) \tag{11}$$

3.3.4. Droplet upwards across transition region ($v_3 < v < v_2$, $C_D = 0.4 + 40/Re$)

According to Eq. (4), there is

$$10(\rho_s - \rho)g + \frac{3\rho}{d}v'^2 + \frac{300\mu}{d^2}v' = -10\rho_s\frac{dv}{dt} \tag{12}$$

3.3.4.1 If $d < \sqrt[3]{\frac{750\mu^2}{\rho(\rho_s-\rho)g}}$, integrating Eq. (12) gives

$$v = \frac{1}{3\rho d}\sqrt{9\times10^4\mu^2 - 120\rho(\rho_s-\rho)d^3g} \times\left(1 - \frac{6\rho d(v_a-u)+300\mu-\sqrt{9\times10^4\mu^2-120\rho(\rho_s-\rho)d^3g}}{6\rho d(v_a-u)+300\mu+\sqrt{9\times10^4\mu^2-120\rho(\rho_s-\rho)d^3g}}\ \exp\left(-\frac{t}{\rho_s d^2}\sqrt{900\mu^2-1.2\rho(\rho_s-\rho)d^3g}\right)\right)^{-1} - \frac{1}{6\rho d}(300\mu + \sqrt{9\times10^4\mu^2 - 120\rho\,(\rho_s-\rho)\,d^3g}) + u \tag{13}$$

And then,

$$h = \left(\frac{1}{6\rho d}\sqrt{9\times10^4\mu^2-120\rho(\rho_s-\rho)d^3g} - \frac{50\mu}{\rho d} + u\right)t + \frac{10\rho_s d}{3\rho} \times\ln\left(\frac{3\rho d(v_a-u)+150\mu}{\sqrt{9\times10^4\mu^2-120\rho(\rho_s-\rho)d^3g}} + \frac{1}{2} - \left(\frac{3\rho d(v_a-u)+150\mu}{\sqrt{9\times10^4\mu^2-120\rho(\rho_s-\rho)d^3g}} - \frac{1}{2}\right) \times\exp\left(-\frac{t}{\rho_s d^2}\sqrt{900\mu^2-1.2\rho(\rho_s-\rho)d^3g}\right)\right) \tag{14}$$

3.3.4.2 If $d = \sqrt[3]{\frac{750\mu^2}{\rho(\rho_s-\rho)g}}$, integrating Eq. (12) gives

$$v = \left(\frac{15\mu t}{d^2\rho_s}\left(u - v_a - \frac{50\mu}{d\rho}\right) - u + v_a\right)\left(1 - \frac{3\rho t}{10d\rho_s}\left(u - v_a - \frac{50\mu}{d\rho}\right)\right)^{-1} + u \tag{15}$$

And then,

$$h = \left(u - \frac{50\mu}{d\rho}\right)t + \frac{10d\rho_s}{3\rho}\ \ln\left(1 - \frac{3\rho t}{10d\rho_s}\left(u - v_a - \frac{50\mu}{d\rho}\right)\right) \tag{16}$$

3.3.4.3 If $d > \sqrt[3]{\frac{750\mu^2}{\rho(\rho_s-\rho)g}}$, integrating Eq. (12) gives

$$v = \left(\left(\frac{10(\rho_s-\rho)gd}{3\rho} - \frac{2500\mu^2}{\rho^2d^2}\right)\left(v_a + \frac{50\mu}{d\rho} - u\right)^{-1} + v_a + \frac{50\mu}{d\rho} - u\right) \times\left(1 + \left(\frac{10(\rho_s-\rho)gd}{3\rho} - \frac{2500\mu^2}{\rho^2d^2}\right)^{-1/2}\left(v_a + \frac{50\mu}{d\rho} - u\right)\ \tan\left(\frac{(0.3\rho(\rho_s-\rho)gd^3 - 225\mu^2)^{1/2}}{\rho_s d^2}t\right)\right)^{-1} + \left(\frac{2500\mu^2}{\rho^2d^2} - \frac{10(\rho_s-\rho)gd}{3\rho}\right)\left(v_a + \frac{50\mu}{d\rho} - u\right)^{-1} - \frac{50\mu}{d\rho} + u \tag{17}$$

And then,

$$h = \left(u - \frac{50\mu}{d\rho}\right)t + \left(\frac{10(\rho_s-\rho)\rho\rho_s^2gd^5 - 7500\rho_s^2\mu^2d^2}{0.9\rho^3(\rho_s-\rho)gd^3 - 675\rho^2\mu^2}\right)^{1/2}\ \ln\left(\cos\left(\frac{t}{\rho_s d^2}\sqrt{0.3\rho(\rho_s-\rho)gd^3 - 225\mu^2}\right) + \left(\frac{10(\rho_s-\rho)gd}{3\rho} - \frac{2500\mu^2}{\rho^2d^2}\right)^{-1/2}\left(v_a + \frac{50\mu}{d\rho} - u\right)\ \sin\left(\frac{t}{\rho_s d^2}\sqrt{0.3\rho(\rho_s-\rho)gd^3 - 225\mu^2}\right)\right) \tag{18}$$

3.3.5. Droplet upwards across laminar region ($v_4 < v < v_3,\ C_D = 24/Re$)

According to Eq. (4), there is

$$\rho_s \frac{dv}{dt} + \frac{18\mu}{d^2} v + (\rho_s - \rho)g - \frac{18\mu}{d^2} u = 0 \tag{19}$$

Integrating Eq. (19) gives

$$v = u - v_s + (v_a + v_s - u)\exp\left(-\frac{18\mu}{d^2\rho_s} t\right) \tag{20}$$

where v_s is Stokes velocity, $v_s = \frac{(\rho_s-\rho)gd^2}{18\mu}$. And then,

$$h = \frac{d^2\rho_s}{18\mu}(v_a + v_s - u)\left(1 - \exp\left(-\frac{18\mu}{d^2\rho_s} t\right)\right) + (u - v_s)t \tag{21}$$

3.3.6. Droplet upwards across transition region ($v_5 < v < v_4,\ C_D = 0.4 + 40/Re$)

The relative velocity of droplet is $v' = u - v$, and the drag force upwards. According to Eq. (4), there is

$$10(\rho_s - \rho)g - \frac{3\rho}{d} v'^2 - \frac{300\mu}{d^2} v' = -10\rho_s \frac{dv}{dt} \tag{22}$$

Eq. (22) can be integrated to

$$v = \frac{1}{3\rho d}\sqrt{9\times10^4\mu^2 + 120\rho(\rho_s-\rho)d^3 g}\left(1 - \frac{6\rho d(u - v_a) + 300\mu + \sqrt{9\times10^4\mu^2 + 120\rho(\rho_s-\rho)d^3 g}}{6\rho d(u - v_a) + 300\mu - \sqrt{9\times10^4\mu^2 + 120\rho(\rho_s-\rho)d^3 g}} \times \exp\left(\frac{t}{\rho_s d^2}\sqrt{900\mu^2 + 1.2\rho(\rho_s-\rho)d^3 g}\right)\right)^{-1} + \frac{1}{6\rho d}\left(300\mu - \sqrt{9\times10^4\mu^2 + 120\rho(\rho_s-\rho)d^3 g}\right) + u \tag{23}$$

And then,

$$h = \left(\frac{1}{6\rho d}\sqrt{9\times10^4\mu^2 + 120\rho(\rho_s-\rho)d^3 g} + \frac{50\mu}{\rho d} + u\right)t - \frac{10\rho_s d}{3\rho} \times \ln\left(\frac{1}{2} - \frac{3\rho d(u - v_a) + 150\mu}{\sqrt{9\times10^4\mu^2 + 120\rho(\rho_s-\rho)d^3 g}} + \left(\frac{1}{2} + \frac{3\rho d(v_a - u) + 150\mu}{\sqrt{9\times10^4\mu^2 + 120\rho(\rho_s-\rho)d^3 g}}\right) \times \exp\left(\frac{t}{\rho_s d^2}\sqrt{900\mu^2 + 1.2\rho(\rho_s-\rho)d^3 g}\right)\right) \tag{24}$$

3.3.7. Droplet upwards across turbulent region ($v_6 < v < v_5,\ C_D = 0.44$)

According to Eq. (4), there is

$$100(\rho_s - \rho)g - \frac{33\rho}{d} v'^2 = -100\rho_s \frac{dv}{dt} \tag{25}$$

Eq. (25) can be integrated to

$$v = 20\sqrt{\frac{(\rho_s-\rho)dg}{33\rho}}\left(1 + \frac{10\sqrt{(\rho_s-\rho)dg} + \sqrt{33\rho}(u - v_a)}{10\sqrt{(\rho_s-\rho)dg} - \sqrt{33\rho}(u - v_a)}\exp\left(\sqrt{\frac{33\rho(\rho_s-\rho)g}{25d\rho_s^2}}\,t\right)\right)^{-1} - 10\sqrt{\frac{(\rho_s-\rho)dg}{33\rho}} + u \tag{26}$$

And,

$$h = \left(10\sqrt{\frac{(\rho_s-\rho)dg}{33\rho}} + u\right)t - \frac{100d\rho_s}{33\rho}\ln\left(\frac{1}{2} - \frac{\sqrt{33\rho}(u - v_a)}{20\sqrt{(\rho_s-\rho)dg}} + \left(\frac{1}{2} + \frac{\sqrt{33\rho}(u - v_a)}{20\sqrt{(\rho_s-\rho)dg}}\right)\exp\left(\sqrt{\frac{33\rho(\rho_s-\rho)g}{25d\rho_s^2}}\,t\right)\right) \tag{27}$$

3.3.8. Droplet upwards across turbulent boundary layer ($v < v_6,\ C_D = 0.1$)

According to Eq. (4), there is

$$100(\rho_s - \rho)g - \frac{7.5\rho}{d}v'^2 = -100\rho_s\frac{dv}{dt} \tag{28}$$

Eq. (28) can be integrated to

$$v = 20\sqrt{\frac{(\rho_s-\rho)dg}{7.5\rho}}\left(1+\frac{10\sqrt{(\rho_s-\rho)dg}+\sqrt{7.5\rho}(u-v_a)}{10\sqrt{(\rho_s-\rho)dg}-\sqrt{7.5\rho}(u-v_a)}\ \exp\left(\sqrt{\frac{7.5\rho(\rho_s-\rho)g}{25d\rho_s^2}}t\right)\right)^{-1} - 10\sqrt{\frac{(\rho_s-\rho)dg}{7.5\rho}} + u \tag{29}$$

And then,

$$h = \left(10\sqrt{\frac{(\rho_s-\rho)dg}{7.5\rho}}+u\right)t - \frac{100d\rho_s}{7.5\rho}\ \ln\left(\frac{1}{2}-\frac{\sqrt{7.5\rho}(u-v_a)}{20\sqrt{(\rho_s-\rho)dg}}+\left(\frac{1}{2}+\frac{\sqrt{7.5\rho}(u-v_a)}{20\sqrt{(\rho_s-\rho)dg}}\right)\exp\left(\sqrt{\frac{7.5\rho(\rho_s-\rho)g}{25d\rho_s^2}}t\right)\right) \tag{30}$$

4. Results and discussion

4.1. Velocity of droplet

When a droplet forms, it will enter the vapor flow with a certain initial velocity. Owing to droplet affected by gravity, buoyancy, and drag force during its ascending in vapor separation space, the velocity of droplet may change with time. Assuming the initial velocity of droplet is $v_0 = 3\,\text{m/s}$, and considering the velocities of vapor flow are $u = 2$ and 0.5 m/s, respectively, the change of velocity of droplet with time are shown in Fig. 5(a and b). In the calculation, all the potential flow regions through which a droplet may pass are considered, and the results are based on their combination.

All the droplets decelerate after entering the vapor flow. Some smaller droplets gradually reach a steady velocity and go out of the evaporator with vapor flow, and some bigger droplets, getting a certain height, stop and descend back to liquid. For the droplet with a certain diameter, the slower the vapor flow, the sooner the droplet gets its final velocity, which is steady upwards or oppositely downwards. The faster the vapor flows, the bigger the diameter of immobile suspended droplet would be, with which the theoretical final velocity would be zero. It corresponds well with the numerical results by Chen et al. [14].

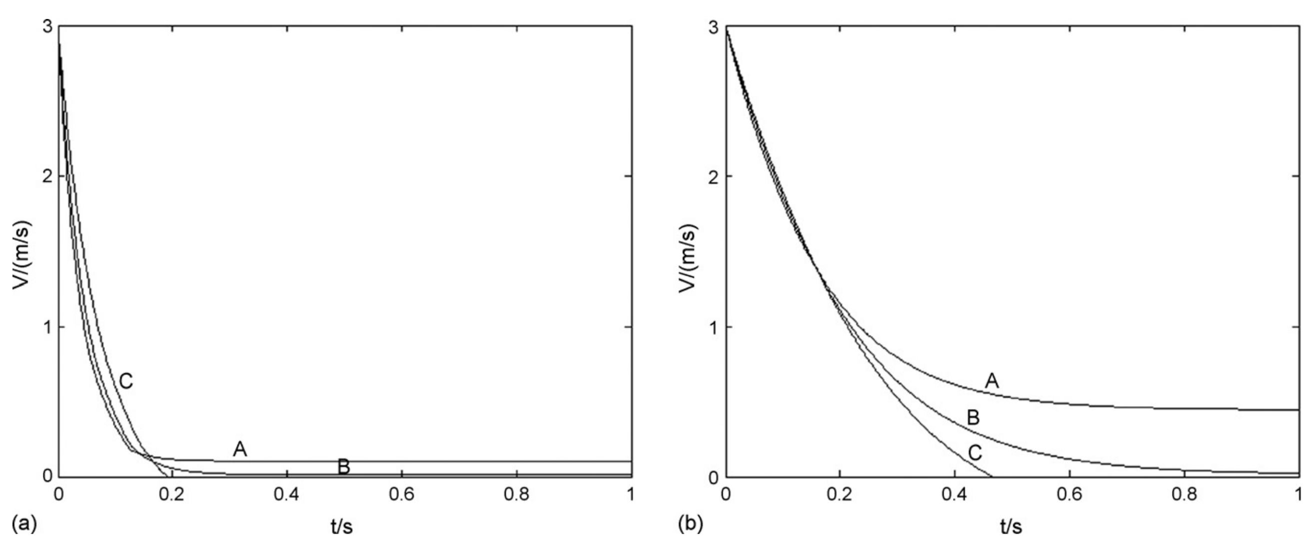

Fig. 5. (a) Variation of velocity of droplet with time: (A) $d = 1.3 \times 10^{-4}$ m; (B) $d = 1.45 \times 10^{-4}$ m; (C) $d = 1.8 \times 10^{-4}$ m; $u = 0.5$ m/s, $v_0 = 3\,\text{m/s}$. (b) Variation of velocity of droplet with time: (A) $d = 2.8 \times 10^{-4}$ m; (B) $d = 3.3 \times 10^{-4}$ m; (C) $d = 3.8 \times 10^{-4}$ m; $u = 2$ m/s, $v_0 = 3\,\text{m/s}$.

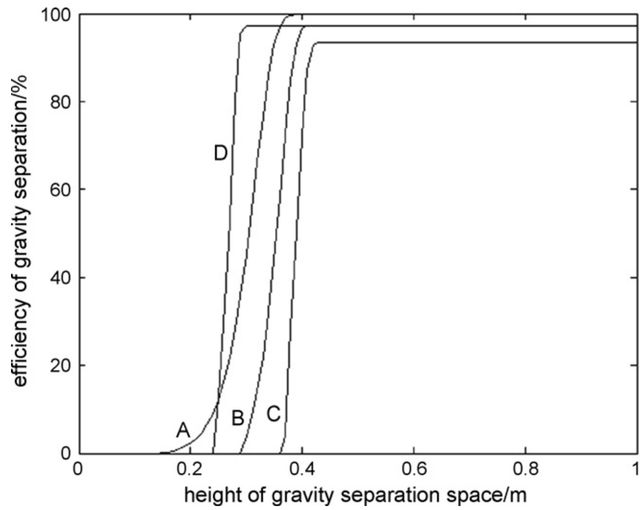

Fig. 6. Variation of separation efficiency with gravity separation height: (A) $u = 0.5$ m/s, $v_0 = 3$ m/s; (B) $u = 1$ m/s, $v_0 = 3$ m/s; (C) $u = 1.3$ m/s, $v_0 = 3$ m/s; (D) $u = 1$ m/s, $v_0 = 2.5$ m/s.

4.2. Separation efficiency

Assuming that the diameter of droplet meets Gauss distribution [14],

$$f(d) = \frac{1}{\sqrt{2\pi}\delta} \exp\left[-\frac{(d-\lambda)^2}{2\delta^2}\right] \tag{31}$$

where

$$d_{\min} \le d \le d_{\max}, \quad d_{\max} = 6 \times 10^{-3}\,\text{m}, \quad d_{\min} = 6 \times 10^{-6}\,\text{m}, \quad \delta = 1 \times 10^{-4}, \quad \lambda = 3 \times 10^{-4}\,\text{m}. \tag{32}$$

If the droplet, of which the diameter is bigger than d_s, can be separated by gravity from the vapor flow, the quantity of discharged liquid in the vapor flow is

$$w_2 = w_1 \frac{\int_{d_{\min}}^{d_x} f(x) x^3\,\mathrm{d}x}{\int_{d_{\min}}^{d_{\max}} f(x) x^3\,\mathrm{d}x} \tag{33}$$

where w_1 and w_2 are the quantity of formed and discharged water in the vapor flow, respectively. The efficiency of separation is defined as the ratio of the quantity of discharged and formed water in the vapor flow. Accordingly,

$$\eta = 1 - \frac{w_2}{w_1} \tag{34}$$

where η is the separation efficiency.

It shows in Fig. 6 that the separation efficiency changes rapidly from minimum to maximum in a small range of gravity separation height. This demonstrates that it is not necessary to increase the gravity separation height after getting the maximum efficiency. It shows in Fig. 6 as well that at the same initial velocity of droplet i.e. $v_0 = 3$ m/s and the same gravity separation height, the faster the vapor flow, the lower the separation efficiency is. With the same velocity of vapor flow, the maximum efficiencies of separation for different initial velocities of droplet are the same, and the faster the initial velocity, the higher space for gravity separation is needed to get the maximum efficiency.

5. Conclusions

A gravity separation model for submerged combustion evaporator is elaborated and its analytical solution is given. Based on this, some major parameters for the separation efficiency of submerged combustion evaporator are discussed, and the following conclusions can be made:

(1) All the droplets decelerate after entering the vapor flow. For the droplet with a certain diameter, the slower the vapor flows, the sooner the droplet gets its final velocity, which is steady upwards or oppositely downwards.
(2) It is not necessary to increase gravity separation height after getting the maximum efficiency.

(3) At the same gravity separation height, the faster the vapor flows, the lower the separation efficiency gets. With the same velocity of vapor flow, the maximum efficiencies of separation for different initial velocities of droplet are the same. And the faster the initial velocity, the higher space for gravity separation is needed to get the maximum efficiency.

Acknowledgement

This research was supported by research funding from the Innovation Foundation of Tsinghua University for PhD Candidate in 2001.

References

[1] N. Swindin, Submerged flame combustion, Trans. Inst. Chem. Eng. 5 (1927) 110–136.
[2] C.F. Hammond, The history and development of submerged combustion, J. Inst. Fuel 4 (1930) 303–325.
[3] R. Williams, R. Walker, Efficient heat transfer by submerged combustion, Gas Eng. Manage. 7 (1997) 32–33.
[4] P.L.C. Lage, F.B. Campos, Advances in direct contact evaporator design, Chem. Eng. Technol. 1 (2004) 91–96.
[5] K.A. Kobe, F.H. Conrad, E.W. Jackson, Evaporation by submerged combustion (I, II), Ind. Eng. Chem. 9 (1933) 984–989.
[6] K.A. Kobe, C.W. Hauge, C.J. Carlson, Evaporation by submerged combustion (III, IV, V), Ind. Eng. Chem. 5 (1936) 589–594.
[7] E.M. Burdick, C.O. Anderson, W.E. Duncan, Application of submerged combustion to processing of citrus waste products, Chem. Eng. Prog. 9 (1949) 539–544.
[8] W.I. Weisman, Applications of submerged combustion in industrial waste treatment, in: 8th Purdue Industrial Waste Conference, Purdue University, USA, 1953, pp. 363–367.
[9] G.L. Kovacs, Promoted oxidation of aqueous ferrous chloride solution, USA patent 4,248,851 (1981).
[10] J.D. Young, E.A. Fischer, Method and apparatus for disposing of landfill produced pollutants, USA patent 4,838,184 (1989).
[11] B.F. Duesel, Leachate evaporation system, USA patent 5,342,482 (1994).
[12] Y. Nie, D. Yue, Y. Xu, Two-stage submerged combustion evaporation process for landfill leachate treatment, CHN patent ZL 03153700.6 (2003) (in Chinese).
[13] S. Liu, Theoretic Analysis for Gravity Separation of Water Droplets in PWR Steam Generator, China Nuclear Technology Report 00, 1996, pp. 1–10.
[14] S. Chen, S. Huang, X. Zhao, A study on the gravity separation of water droplets in steam generators for PWR, J. Huazhong Univ. Sci. Technol. 1 (1997) 69–71 (in Chinese).